Available online at www.sciencedirect.com

SCIENCE DIRECT®

Tectonophysics 389 (2004) 111–124

TECTONOPHYSICS

www.elsevier.com/locate/tecto

Hawaiian hot-spot swell structure from seafloor MT sounding

Steven Constable[a,*], Graham Heinson[b,1]

[a]Scripps Institution of Oceanography, La Jolla, CA 92093-0225, USA
[b]School of Earth and Environmental Sciences, University of Adelaide, Adelaide, Australia

Received 26 March 2003; accepted 23 July 2004

Abstract

Seafloor magnetotelluric (MT) data were collected at seven sites across the Hawaiian hot spot swell, spread approximately evenly between 120 and 800 km southwest of the Hawaiian-Emperor island chain. All data are consistent with an electrical strike direction of 300°, aligned along the seamount chain, and are well fit using two-dimensional (2D) inversion. The major features of the 2D electrical model are a resistive lithosphere underlain by a conductive lower mantle, and a narrow, conductive, 'plume' connecting the surface of the islands to the lower mantle. This plume is required; without it the swell bathymetry produces a large divergence of the along-strike and across-strike components of the MT fields, which is not seen in the data. The plume radius appears to be less than 100 km, and its resistivity of around 10 Ωm, extending to a depth of 150 km, is consistent with a bulk melt fraction of 5–10%.

A seismic low velocity region (LVR) observed by Laske et al. [Laske, G., Phipp Morgan, J., Orcutt, J.A., 1999. First results from the Hawaiian SWELL experiment, Geophys. Res. Lett. 26, 3397–3400] at depths centered around 60 km and extending 300 km from the islands is not reflected in our inverse model, which extends high lithospheric resistivities to the edge of the conductive plume. Forward modeling shows that resistivities in the seismic LVR can be lowered at most to 30 Ωm, suggesting a maximum of 1% connected melt and probably less. However, a model of hot subsolidus lithosphere of 10^2 Ωm (1450–1500 °C) within the seismic LVR increasing to an off-swell resistivity of $>10^3$ Ωm (<1300 °C) fits the MT data adequately and is also consistent with the 5% drop in seismic velocities within the LVR. This suggests a 'hot, dry lithosphere' model of thermal rejuvination, or possibly underplated lithosphere depleted in volatiles due to melt extraction, either of which is derived from a relatively narrow mantle plume source of about 100 km radius. A simple thermal buoyancy calculation shows that the temperature structure implied by the electrical and seismic measurements is in quantitative agreement with the swell bathymetry.

Keywords: Plumes; Seafloor conductivity; Hawaii swell; Magnetotellurics

1. Introduction

Two prominent features mark the passage of oceanic lithosphere over a hot-spot. The first is the

* Corresponding author. Fax: +1 858 5348090.
E-mail addresses: sconstable@ucsd.edu (S. Constable), Graham.Heinson@adelaide.edu.au (G. Heinson).
[1] Fax: +61 8 83034347.

0040-1951/$ - see front matter © 2004 Elsevier B.V. All rights reserved.
doi:10.1016/j.tecto.2004.07.060

initiation of oceanic volcanism leading to a chain of islands or seamounts. The second is the generation of a 1 km high, 1000 km wide bathymetric swell around the volcanic island chain. The origin of hotspot swells is still largely unknown. At least three different mechanisms have been proposed for swell generation; (i) thermal reheating (rejuvenation) of the lithosphere within a 1000 km region centered on the hotspot (Crough, 1978; Detrick and Crough, 1978); (ii) compositional underplating of depleted mantle residue from hotspot melting (Robinson, 1988; Phipps Morgan et al., 1995); and (iii) dragging of hot plume asthenosphere by the overriding lithosphere (Sleep, 1990). The primary reason for the multiplicity of theoretical models is that there are few geophysical constraints on the structure of the lithosphere and sub-lithosphere beneath a swell (Sleep, 1990). Constraints from both global and regional seismic studies are poor, since most current global models cannot reliably resolve features of diameters less than 500 km.

The Hawaiian swell is an excellent place to study the interactions of a mantle plume with oceanic upper lithosphere; large volumes of melt are being produced and the area is geographically isolated from coastlines, mid-ocean ridges, and subduction zones. The Hawaiian islands are almost in the center of the Pacific plate and are surrounded by lithosphere of 90–110 Ma age moving at a velocity of 83 mm/year (Gordon and Jurdy, 1986). In 1997, the SWELL (Seismic Wave Exploration of the Lower Lithosphere beneath the Hawaiian swell) experiment took place, a pilot study to deploy long period hydrophones across the Hawaiian swell (Laske et al., 1999). We were able to piggyback the cruise and collect data from seven marine magnetotelluric (MT) instruments deployed in coordination with the seismic hydrophones between April and December 1997 from the RV Moana Wave. Fig. 1

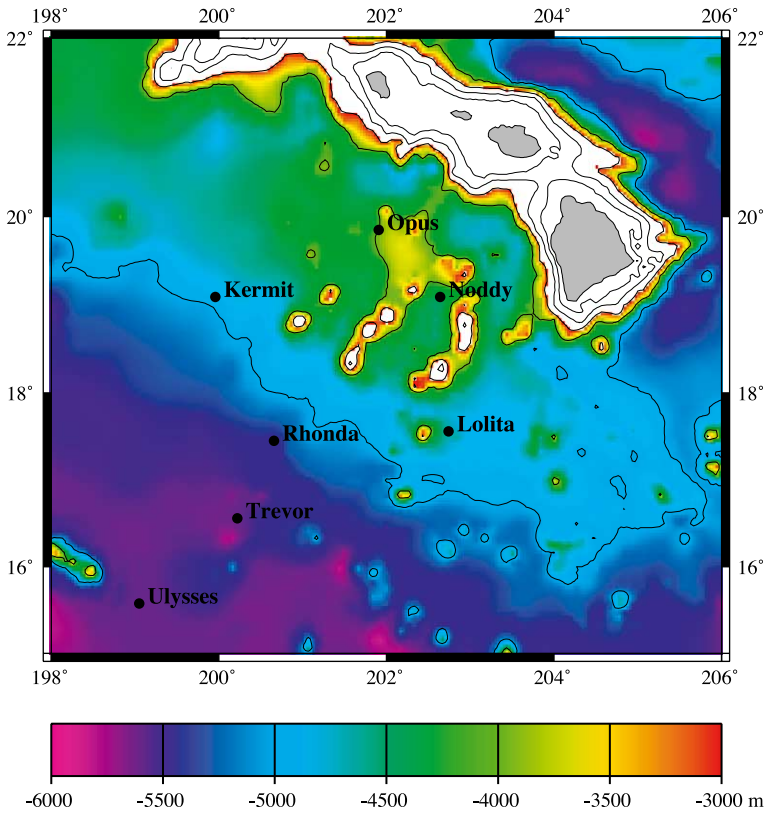

Fig. 1. Location of the seven MT instruments used in the experiment (see also Table 1). All returned magnetic data, but only one channel of electric-field data was recorded at site L. The edge of the swell is approximately given by the 5000 m depth contour.

Table 1
Instrument locations and depths

Instrument	Site	Latitude	Longitude	Depth (m)	Data
Opus	O	19°50.98	158°05.43	4350	E/B
Noddy	N	19°05.42	157°21.53	4570	E/B
Lolita	L	17°33.60	157°15.60	4760	B
Kermit	K	19°03.60	160°26.71	4950	E/B
Rhonda	R	17°26.98	159°20.40	5290	E/B
Trevor	T	16°33.63	159°46.80	5640	E/B
Ulysses	U	15°34.88	160°57.05	5620	E/B

shows the swell (bounded by the 5000 m depth contour) and locations of MT sites (listed in Table 1). Location of sites was primarily chosen for seismic surface-wave analyses, and hence a hexagonal array with a central instrument at the ODP Borehole 843B was used (Laske et al., 1999). However, MT sites were positioned so that four MT responses were obtained above the swell (<5000 m water depth), and three in the deeper ocean to the south of the swell, with site spacing of the order of 250 km. All instruments were successfully recovered with data.

2. Data

The MT method requires the simultaneous time-series measurement of orthogonal components of magnetic (Bx, By, and Bz) and electric (Ex and Ey) variational fields that result from large-scale ionospheric electric currents and temporal variations in magnetosphere morphology. Typical deep-ocean MT observations are made in a bandwidth of 10^3 to 10^5 s, limited by the high electrical conductance of the ocean at short periods, and source-field non-uniformity and contamination by oceanographic sources at long periods. Short-period magnetic fields are attenuated to a greater extent than electric fields because they have a higher reflection coefficient over a resistive seafloor (e.g. Constable et al., 1998). Thus the resistive nature of 100 Ma lithosphere reduces the magnitude of the seafloor magnetic fields and exacerbates the difficulty in recording MT fields at higher frequencies, resulting in data with a maximum sensitivity to structure between 10 and 400 km into Earth.

Magnetic and electric field time series of 8 months duration sampled every 20 s were processed with the robust remote-reference scheme of Chave and Thomson (1989) using reference data from the shallowest sites N or O. Typical processing errors are less than 5% in the bandwidth 10^3 to 4×10^4 s, and 10% or greater at shorter or longer periods. Site L, which only recorded one channel of electric field, was processed with electric fields from site K, which is in a similar water depth.

The ratio of orthogonal horizontal components of E and B in the frequency domain is a measure of Earth's electrical resistivity over a volume that increases with depth and width as the period increases. With pairs of orthogonal E and B fields, MT responses may be obtained in two polarizations, or modes. Above 1D layered structures the two MT modes are identical, but for two-dimensional (2D) structures MT fields may be rotated to modes of electric field parallel to strike (TE mode) and perpendicular to strike (TM mode). More complex 3D structures will have non-uniform MT responses that cannot be simply decomposed to TE and TM modes. The ratio of vertical magnetic field (Bz) to the horizontal fields (Bx and By), known as GDS, or tipper, responses, also provides a measure of lateral changes in resistivity. If no lateral changes exist, Bz will be zero for periods in the bandwidths stated above. Although non-planar source-field geometry may produce vertical fields, the latitude of the experiment (16–20°N) is well away from the geomagnetic electrojet and auroral zones that would otherwise cause such effects. Furthermore, the large conductivity contrast between air and seawater results in a well-behaved seafloor MT response even in the presence of source-field inhomogeneity. For example, Heinson et al. (2000) were able to process seafloor MT data effectively at high latitudes during auroral activity.

Data were analyzed using the decomposition methods of Groom and Bailey (1989) and the Mohr circle method of Lilley (1998). It is presumably difficult to maintain the charge buildup necessary for near-surface galvanic distortion or static shift on the seafloor because of the high conductivity of seawater. However, decomposition methods provide useful tools for the determination of strike and assessment of dimensionality. In this case, off-diagonal terms (associated with 3D induction) were an order of magnitude smaller than the diagonal (2D) terms, and azimuths were found to be generally independent of period, at $61\pm10^\circ$ west of geographic north. Thus, induction

(and galvanic current flow) appears predominantly 2D at all MT sites, with an azimuth orientated parallel to the strike of the 5000 m contour (the edge of the swell; Fig. 1) and the islands. At each site, the MT fields were rotated to the dominant 2D azimuth determined by decomposition, and we define the TE mode to be parallel to edge of the swell, and the TM mode to be perpendicular. Fig. 2 shows all the processed MT

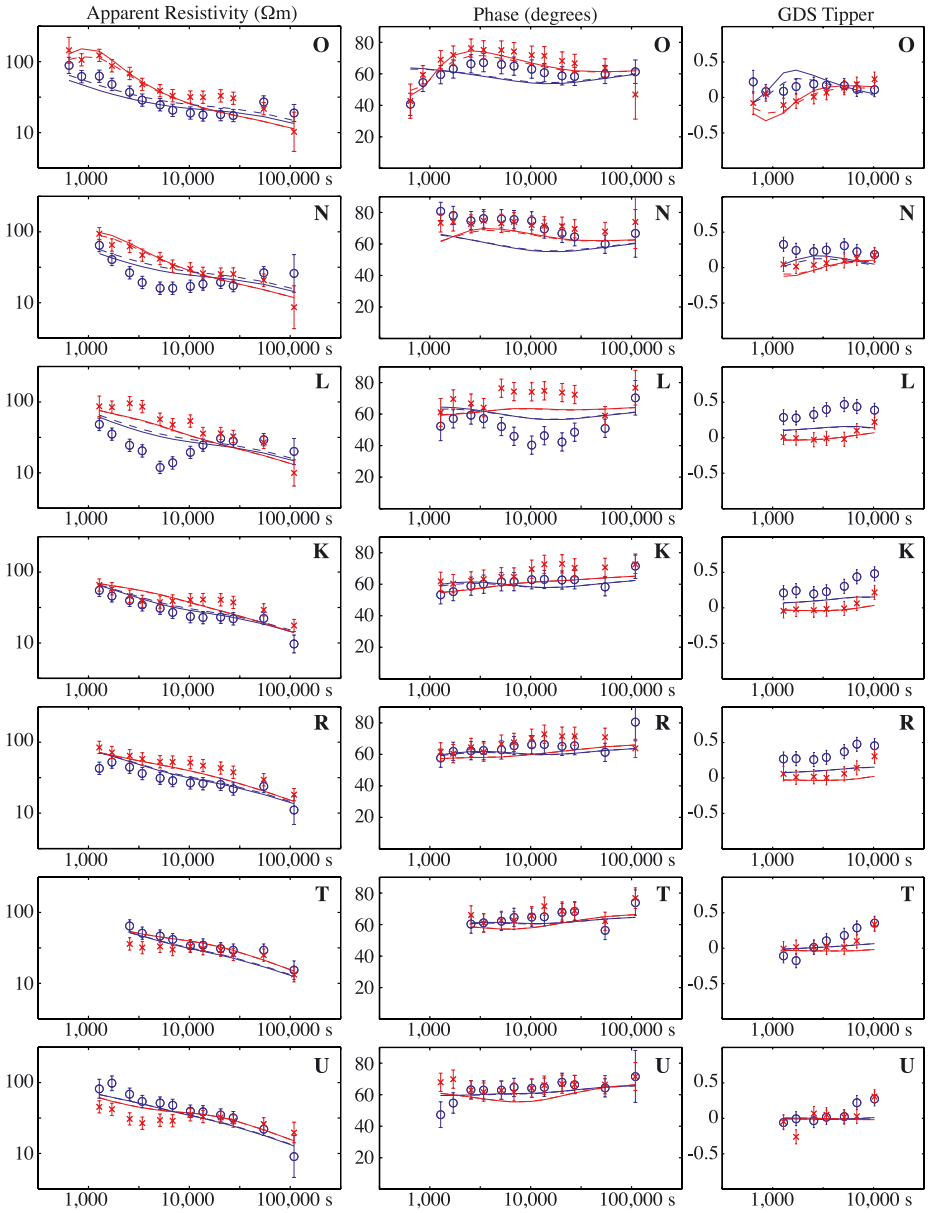

Fig. 2. MT response curves for all sites, ordered from northeast (O) to southwest (U). For each site, the two modes are TE shown by red '×' (electric fields parallel to bathymetry and island chain) and TM shown by blue '○' (electric fields perpendicular). For the GDS tipper data, the real component is shown as blue '○', and the quadrature (imaginary) component by red '×'. Data are shown with one standard deviation error bars for a 20% error floor in resistivity. Solid lines represent the response of the 2D inversion shown in Fig. 4, and the broken lines show the response of the same model but with water depth over the island chain increased by 400 m.

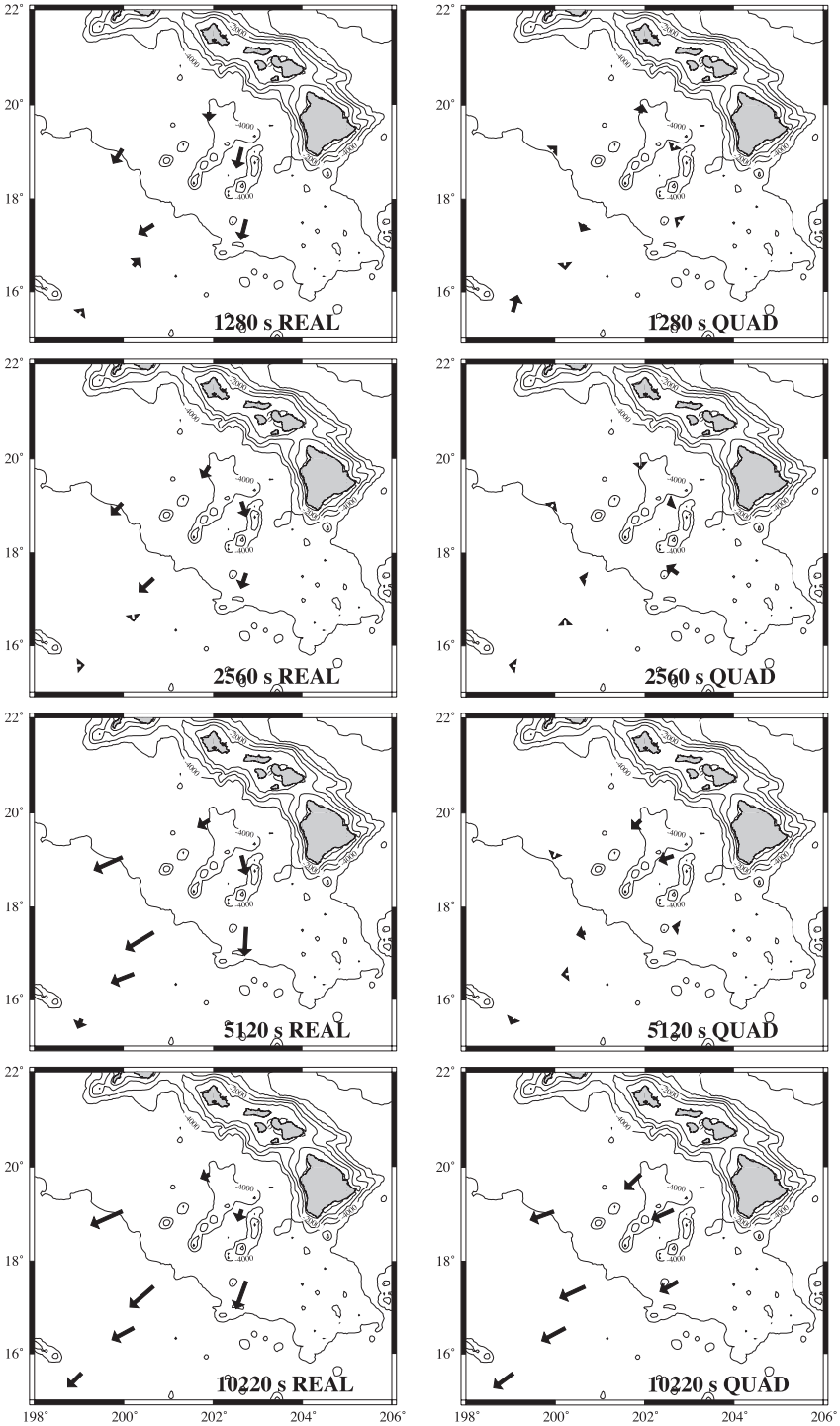

Fig. 3. Parkinson real and quadrature arrows plotted on a map of seafloor topography at four periods of induction. The largest arrows are about 0.6—see Fig. 2 for quantitative data and error bars.

responses. Apparent resistivities are smaller in the TM mode, particularly at sites closest to the islands (O and N), as might be expected from the classical geomagnetic coast (or island) effect. For site O, the offset in apparent resistivity between the two modes is suggestive of a static-shift effect but, as we argue above, this is unlikely on the seafloor, and site O phases are different at all periods, suggesting inductive, rather than galvanic, effects. Probably it is the effect of the islands and bathymetry that accounts for the anisotropy between modes; data from site U, furthest from the islands, are more isotropic, particularly at long periods.

The TM mode resistivity is most obviously influenced by the islands' geomagnetic coast-effect, increasing in resistivity with distance from Hawaii. Greater than 600 km from the islands, TE and TM modes are almost equal, indicating an approximately 1D response. On the other hand, TE apparent resistivities, much less affected by the island bathymetry, are higher for the sites on the swell, and reduce significantly off-swell. A similar response can be seen in the GDS tipper values. Fig. 3 shows real and quadrature Parkinson induction arrows (in the sign convention of Lilley and Arora, 1982) at four periods superimposed on island and seafloor topography. The largest response in the real (in-phase) tippers is at the edge of the swell (about 400 km from the islands), and surprisingly small close to the islands where a larger response might be expected. Quadrature (out-of-phase) tippers show a more uniform response, changing sign from negative to positive at about 6×10^3 s period at all sites, and are generally much smaller than the real tipper components. All real arrows are orientated approximately perpendicular to the swell topography and towards the deep ocean. At periods longer than 10^4 s, quadrature arrows are similar in amplitude (≈ 0.3) and all orientated towards the southwest. The explanation for such behaviour is not clear. One possible reason is source-field inhomogeneity, but we have noted above that this is unlikely. Although the morphology of seafloor MT data is not always the same as for land-based MT, vertical fields are generated by lateral changes in resistivity structure, as on land. One of the largest such features is the coast or bathymetry, and normally very large vertical fields are observed, for example, at the base of the continental slope. It is possible that in this case an ocean basin scale coast-effect may be responsible for the long-period GDS response (Heinson and Constable, 1992).

3. Inversion

Although MT sites are located at various distances and azimuths from the active volcanism of the islands, the orientation of the swell is approximately 2D and parallel to the direction of motion. Thus, a 2D Occam's inversion (deGroot-Hedlin and Constable, 1990) of the sites was carried out as a function of distance from the island chain. Seabed topography was included as a discrete set of topographic ramps of 200 m separated by 100 km, exploiting the triangular elements of Wannamaker et al. (1986) finite element forward code used by the inversion. The island chain is represented by a 150-km-wide block that comes within 300 m of the sea-surface. Approximating topography and sites to mesh nodes was not simple, as clearly the sites are not orientated along a single line. Local topographic variations (such as the seamounts close to site N) were not included. The plume is undoubtedly 3D, but as the plume-width is probably of the order of 100 km, and the nearest sites (O and N) are some distance away, we can justify the 2D approach. Simpson et al. (2000) considered the dimensionality of a possible plume by analyzing daily variations in the magnetic field at two islands, but such sparse data lack the ability quantify lateral extent. Errors associated with the response function estimation procedure and departure from 2D geometry were modeled by assigning a noise floor of 20% error in resistivity, 5.8° in phase, and 0.1 in GDS data.

The maximally smooth Occam inversion was able to fit the entire data set (both modes of resistivity, phase, and GDS) to rms=1.35. Fig. 4 shows a smooth resistivity model fitting the data to rms=1.40, and Fig. 2 shows the fits of this model to the data set. We see more anisotropy in the MT response (a difference between the TE and TM modes) close to the islands, but not as much as one would expect from such topography. The fit to site L, processed without local electric fields, is poor, and other systematic misfits are evident in the data set, but the general features of the responses are reproduced. As we shall see, site O, which is fairly well fit by the model, carries most of

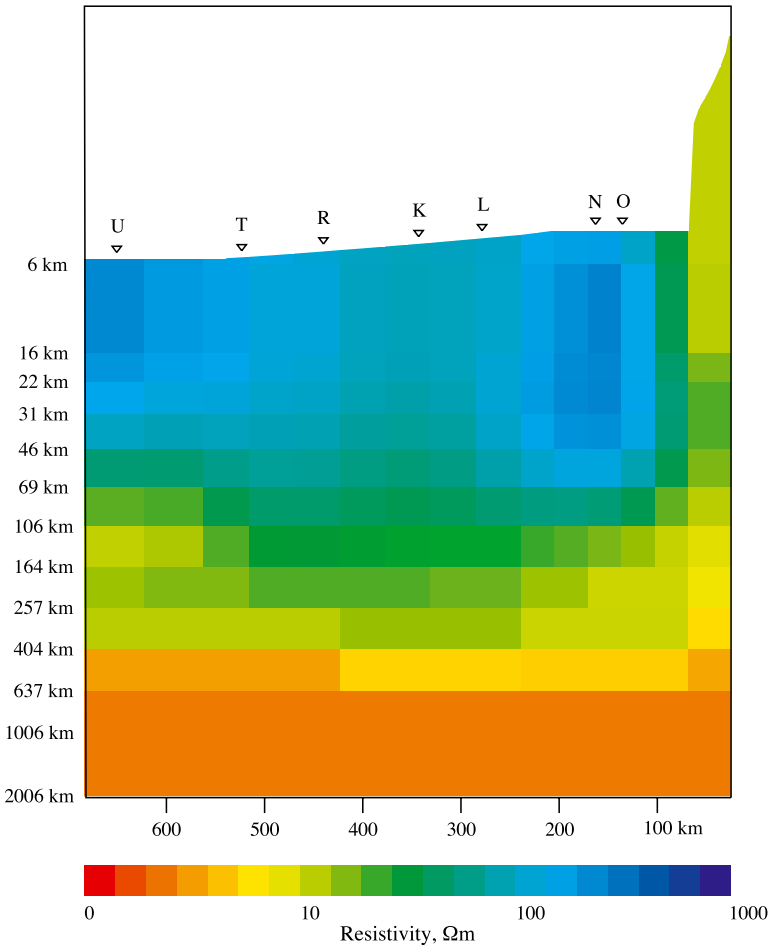

Fig. 4. Two-dimensional smooth inversion of MT and GDS data from the seven marine sites. The island chain is represented by a ridge coming to within 300 m of the sea surface, and the model east of the islands is terminated with seawater layer (not shown here).

the information about geologically interesting structure, so our interpretation is moderately robust to misfits at the other sites.

The model in Fig. 4 shows a surprising uniformity in resistivity across the swell. The dominant features of the model are an increase in conductivity with depth at around 400–1000 km, well known from analysis of long-period magnetic observatory data and associated with the phase changes in olivine in the upper mantle and to perovskite/magnesiowustite in the lower mantle (e.g. Xu et al., 2000), and increased conductivity immediately below the island chain, suggestive of a combination of high temperatures, melt, and seawater-filled porosity (i.e. a mantle plume and associated surface volcanism). To a depth of 100 km away from the islands, the lithosphere is relatively uniform at $\approx 10^2$ Ωm. The resistivity of this lithospheric layer is almost certainly underestimated, because MT has poor sensitivity to resistive layers embedded in conductive structure (represented here by the oceans and lower mantle). We note that this layer derives from depleted mantle at mid-ocean ridges, and hence is probably mostly anhydrous. Constable and Cox (1996) argue, based on their controlled source EM experiments, that at least 10^4 Ωm is typical for cool, olivine-rich lithosphere at temperatures less than 600 °C, well below the mantle solidus. The MT method, on the other hand, can only

quantify the resistivity of such features by means of vertical TM mode current flow, forced by lateral conductivity contrasts such as coastlines. However, in this case the islands lack a strong TM response as a result of their low resistivity.

4. Effect of 3D bathymetry

Implicit in the assumption of the 2D modeling is that structure extends infinitely in the direction of strike. Clearly, this is not the case for the Hawaiian islands. Whilst the chain of islands extends to the northwest for many hundreds of kilometres, there is an abrupt change in bathymetry to the south of Hawaii (the big island), with water depths greater than 5000 m within 50 km of the coastline (Fig. 1). Between the islands water depth reaches up to 1000 m. Additionally, seamount chains around sites O and N have a strike that is approximately orthogonal to the islands.

With only seven sites, it is not realistic to develop a fully three-dimensional (3D) model of the Hawaiian islands bathymetry and a conductive plume. However, judicious use of thin-sheet modeling (McKirdy and Weaver, 1984; McKirdy et al., 1985) permits a study of the effects of bathymetry at the seafloor MT sites. A thin-sheet model was developed that spanned the area shown in Fig. 1 (but extended to latitude 23°N) to yield an area of 6° by 6°. Bathymetry data from the ETOPO30 data set with 5′ resolution (or approximately 9 km grid nodes) were used, to yield 97 by 97 nodes in the model. Conductance of the sheet was determined by the product of seawater conductivity (3.2 S/m) and the water depth; for areas above sea level, the conductance was fixed at 250 S for an island resistivity of 20 Ωm and a 5-km thickness. Beneath the sheet, a 1D layered structure was used from the inversion profile beneath the outermost sites U and T. In this model, a 1 km layer of sediments and fractured basalt with resistivity 10 Ωm overlies a crust and mantle resistivity of 10^4 Ωm to a depth of 50 km. A rapid decrease in resistivity to 50 Ωm to a depth of 120 km and then 10 Ω to 670 km terminates the model.

Modeling of periods from 10^3–10^4 s shows that at sites several hundred kilometres from the islands, MT responses show only a small bathymetric signature, mostly associated with the gentle gradient in seafloor topography. The thin-sheet response is consistent with the MT observations, as shown in Fig. 2 for site U, in which orthogonal modes of induction are almost the same. On the other hand, sites O and N are within 200 km of the island chain to the northeast, but at least twice that distance from southeastern edge of the big island where the bathymetry rapidly changes. Thin-sheet responses at sites O and N show dominantly 2D induction, with strike aligned with the trend of the Hawaiian island chain. The scale-length of effects of smaller seamounts is comparable to the size of the seamount, but is limited by the resolution of the grid. From the thin-sheet models, the biggest effect of local seabed topography occurs at site N, which is located between two seamount chains, and this could account for the poor fit at this site (Fig. 2). From our distortion analysis, site N exhibits the largest departure from a 2D response. These thin-sheet model results are consistent with studies by Wannamaker et al. (1984) which showed that 3D bodies can be modeled with a 2D algorithms provided that the distance from the observation sites to the body is smaller than the length of the body.

Although thin-sheet modeling shows that large-scale bathymetry does not create significant 3D effects, there remains the question of the variation in water depth between the islands, particularly since the role of the island chain in generating a TM mode is a critical element of our interpretation. We have taken an average water depth of 300 m for our 2D model, while in reality the bathymetry varies from a little over 1 km to nothing on the islands. We can test how sensitive our 2D modeling is to this approximation by changing the water depth in our model, from 300 to 700 m. Fig. 2 shows the effect of this; there is almost no difference in the MT response at the deeper sites. At the closest site (O) there is some effect at periods shorter than 10,000 s. Although the overall misfit across the data set increases from rms=1.40 to 1.41 (a statistically insignificant amount), qualitatively the fit appears slightly better for this site. We conclude that the 3D pattern of variable water depth between islands does not have a significant effect on our data.

5. Forward modeling

While the inversion produces a good fit to the data, forward models are used to test the necessity of

features in the inverse model, and compatibility with other geophysical data.

5.1. Requirement for a plume

We interpret the conductive feature below the island chain to be a mantle plume, even though the 2D model representation would not normally be appropriate for such a 3D feature. A conductive path through the resistive oceanic lithosphere under the islands is required to reduce the magnitude of TE/TM mode anisotropy. It is this effect on the seafloor MT data that is important, rather than exact details of geometry or location. We have no constraint on how far the conductive feature extends northeast of the island chain, but the MT data constrain the southwest side to lie outside the array. Our conclusion that the feature is narrow is thus based on an assumption of symmetry across the Hawaiian chain.

To demonstrate that the conductive plume is required by the data, a forward model was run in which the low resistivities beneath the islands were replaced by 10^2 Ωm material to a depth of 70 km. This model increases the data misfit to rms=2.55 overall, and, as shown in Fig. 5, the misfit to the station closest to the islands is unacceptable.

We are not the first to suggest an electrically conductive plume beneath Hawaii. An inversion of land MT and GDS data from Oahu in the period range 10^4–10^7 s by Larsen (1975) and Neal et al. (2000) showed similar resistivities to our model; 1–10 Ωm to depths of 700 km. Simpson et al. (2000) also find evidence for lower resistivities beneath the island of Hawaii where volcanism is current, but their analysis has almost no lateral resolution; our study is the first to provide measurement sites with a significant lateral extent, allowing the size of the plume to be estimated.

5.2. Compatibility with the seismic model

Laske et al. (1999), on analysing surface wave seismic data from the SWELL experiment, find a region of slower shear-wave velocities centred around 70 km depth and extending over 300 km from the islands. Our inversion shows no evidence of this

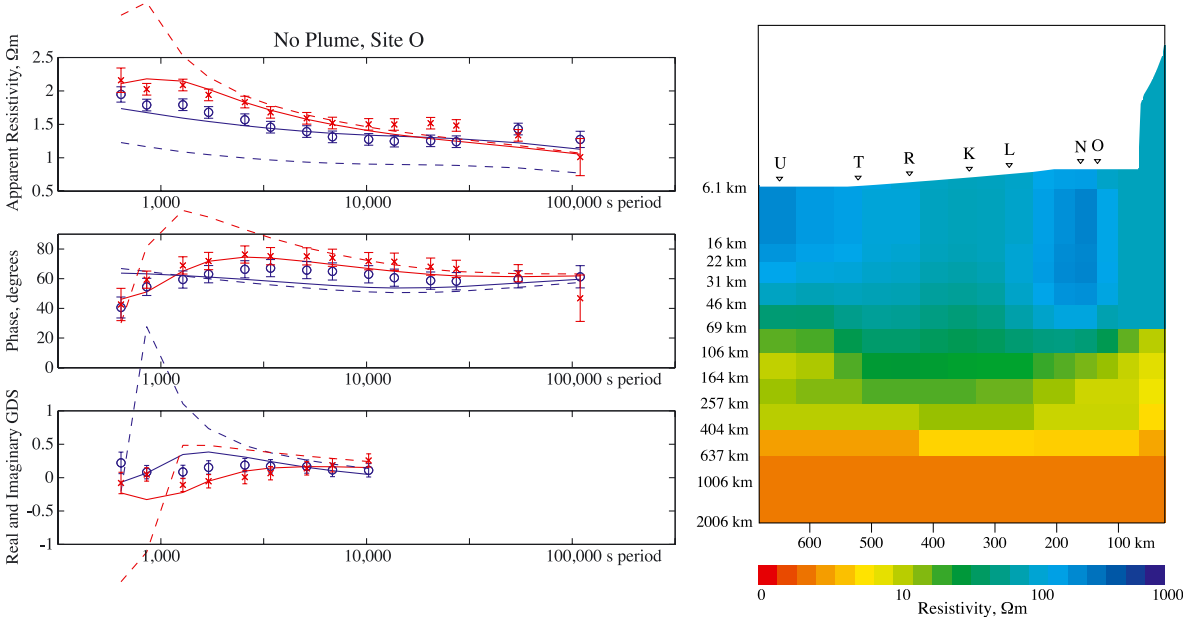

Fig. 5. Model (right) in which the conductive plume is removed from the inverted model (right) and the fit to the nearest site, O (broken lines in left plot). Solid lines on the data plot show the fits of the unperturbed inversion model of Fig. 4. It can be seen that the fit to the data is completely corrupted, providing confidence in the existence of the electrical plume.

feature in the resistivity data, and indeed this region is the most resistive part of the model. This increased resistivity is likely a result of better quality high frequency data from the instruments in shallower water than a real feature of the lithosphere, but nevertheless the implication is that the lower seismic velocities do not result from partial melting, which would increase conductivities dramatically. To test how conductive this region could be made without compromising data fits, a decreased resistivity region was included where the seismic shear wave velocities were below 4.3 m/s (Fig. 6). Any decrease in the resistivity of this region below 10^2 Ωm degrades the fit to the data; by the time the resistivity is reduced to 30 Ωm the fits are significantly poorer (rms=1.58). A further decrease in resistivity to 10 Ωm produces an unambiguous misfit (rms=2.35), exemplified in Fig. 7 for site O.

5.3. Thermal anomaly

If not partial melt, then perhaps a thermal anomaly causes the low seismic velocities beneath the swell. Our lithospheric resistivities of 100–300 Ωm are consistent with an essentially dry olivine rock of 1400–1500 °C (Fig. 8). Although these resistivities extend across the model to the southwestern edge, we do not expect the entire lithosphere to have this temperature and resistivity. We know that normal oceanic lithosphere is much more resistive than 100 Ωm (Constable and Cox, 1996), and we have already noted that the seafloor MT method is not sensitive to such highly resistive structure. We thus tested the model shown in Fig. 7, maintaining a resistivity of 10^2 Ωm within the seismic LVZ, and increasing the lithospheric resistivity outside the LVZ to 1000 Ωm. The thickness of this electrical lithosphere is set at 60 km, based on the controlled source EM work of Constable and Cox (1996). We have, of course, maintained the electrical plume necessary to preserve the data fits.

The statistical misfit associated with this model is rms=1.58, a small but nevertheless significant decrease in acceptability. However, the fit to our benchmark site in shallow water, shown in Fig. 7, is still qualitatively good and in some respects

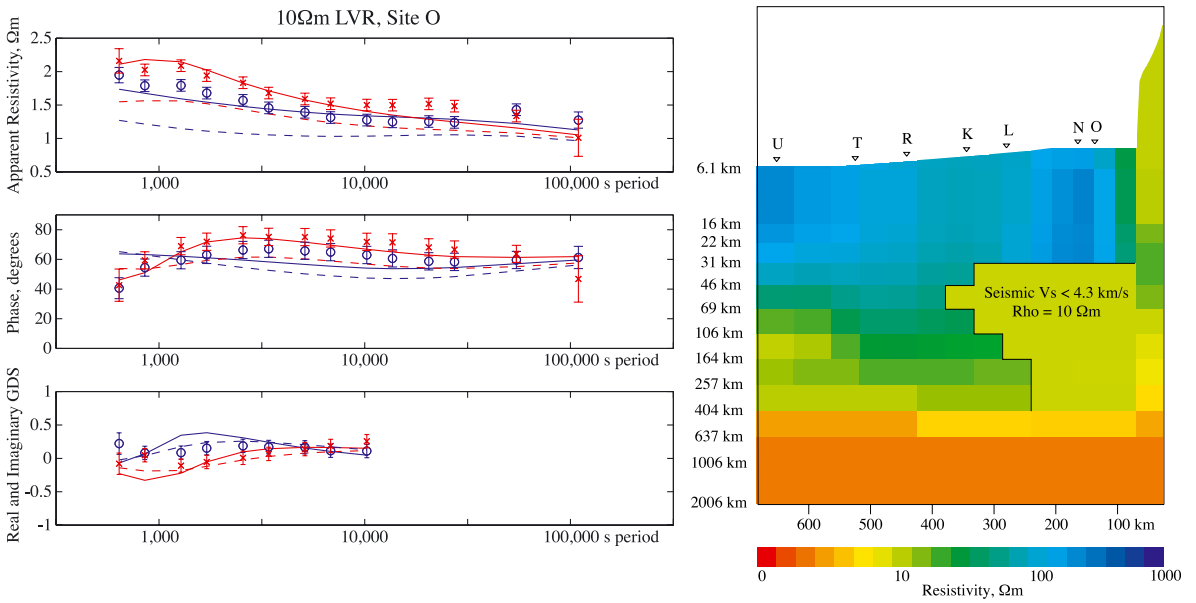

Fig. 6. Model (right) in which the region with lower seismic shear wave velocity (less than 4.3 m/s) is replaced by resistivities of 10 Ωm (right) and fits to the nearest site, O (left). Solid lines show the response of the inversion model of Fig. 4, while broken lines show the response of the modified model. Although the effect is not as dramatic as removing the plume, this modification of the inverse model also degrades the fit to the data.

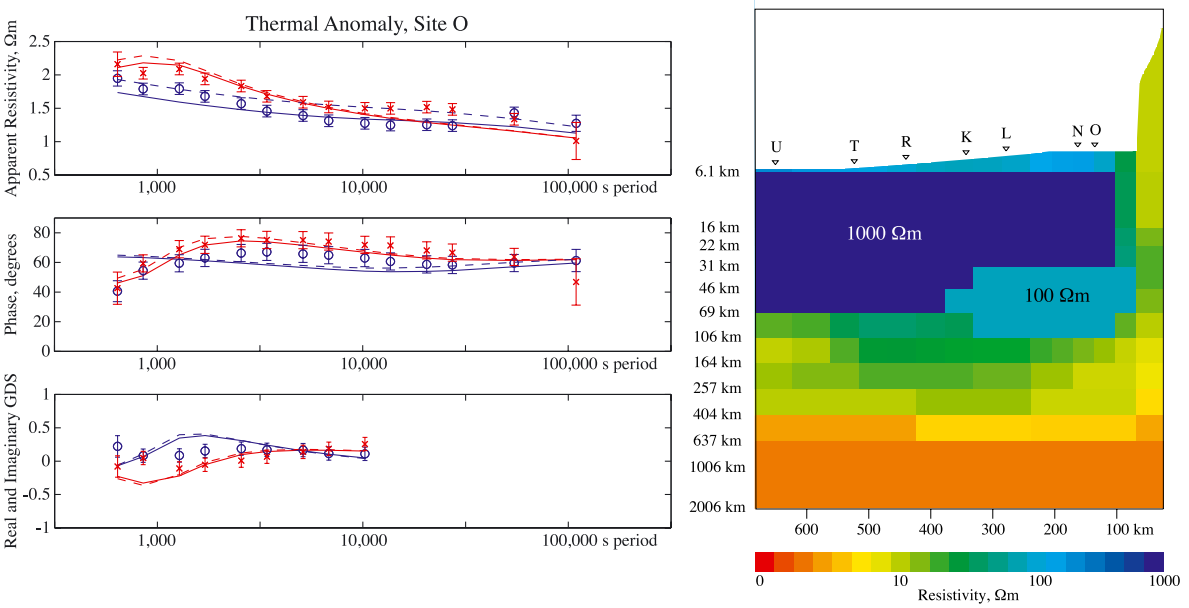

Fig. 7. Model (right) in which the region with lower seismic shear wave velocity (less than 4.3 m/s) is maintained at 10^2 Ωm while the resistivity of the surrounding lithosphere is increased to 10^3 Ωm, representing a thermal anomaly associated with the LVR. The data misfit associated with this model is, from a statistical sense, a barely acceptable 1.58, but as can be seen from site O (left), provides a good qualitative fit to the data.

might be considered better than the smooth inversion. One could expect that small adjustments to the geometry of our thermal model could restore the data misfit while preserving the underlying concept of a hot, dry swell anomaly surrounded by normal lithosphere.

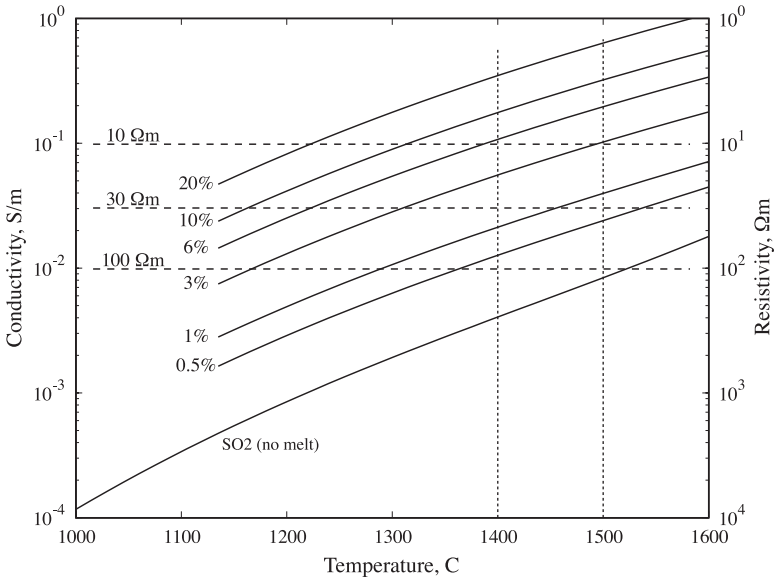

Fig. 8. Predictions for mantle conductivity based on measurements of subsolidus olivine by Constable et al. (1992) and melt by Tyburczy and Waff (1983), using a binary mixing model of well-connected melt along grain-edge tubes.

6. Discussion

In our efforts to explain the origin of the Hawaiian swell, it is natural to ask if the thermal anomaly represented by Fig. 7 is consistent with observed bathymetry. Taking the simple model of Sleep (1990), thermally supported bathymetry is given by

$$\beta = \Delta d \Delta T \alpha$$

where Δd is thickness of the thermal layer supporting the bathymetry, ΔT is the temperature anomaly, and α is the thermal expansion coefficient of the mantle, which here we take to be that of olivine, or approximately 3×10^{-5} C^{-1} (Ribe and Christensen, 1999). If we take the temperature inside our thermal anomaly to be 1400 °C, and the temperature of the surrounding lithosphere to be given by an oceanic geotherm appropriate for 90 My age, then Table 2 provides estimates of ΔT, Δd and β for each layer of the resistivity model between 31 km, where the anomaly starts, and 164 km where the temperature in the anomaly reaches that of the geotherm. If we sum the cumulative effects, we arrive at a total buoyant bathymetry of 1326 m, which agrees well with the difference in depth of our deepest and shallowest instruments (1270 m, Table 1).

High resistivity in the uppermost 50 km suggests uniform temperature gradients across the swell, consistent with seafloor heat-flow measurements that show little variation with location (von Herzen et al., 1982, 1989). Therefore, as for the seismic surface-wave analyses of Laske et al. (1999), the resistivity model does not support the concept of lithosphere thinning and reheating as proposed by Detrick and Crough (1978). Below the swell, resistivity is of order 100 Ωm or higher to depths of 60–160 km. A similar structure was determined beneath the Society Islands hot-spot by Nolasco et al. (1998). Plume temperatures are estimated to be 1500 °C at a depth of 100 km, and the excess temperature of the asthenosphere beneath the swell (assumed to be 100 km thick) is predicted to be 200 to 300 °C (Sleep, 1990). A high temperature asthenosphere over depths of 60 to 160 km beneath the swell is supported by seismic surface-wave analyses (Laske et al., 1999).

Table 2
Thermal buoyancy calculation

Model depth, km	ΔDepth	Geotherm, °C	ΔT, °C	β, m
31–46	15	500	900	405
46–69	23	800	600	414
69–106	37	1100	300	333
106–164	58	1300	100	174
			total	1326

Forward modeling shows that the region of seismic low velocities cannot have a resistivity much lower than 100 Ωm, and can in fact be significantly more resistive. This sub-swell asthenospheric resistivity is consistent with laboratory measurements on olivine (SO2 model) between 1400 to 1500 °C (Constable et al., 1992) and the thermal models of Heinson and Constable (1992) for 100 Ma seafloor. Even at the lower bounds of permissible resistivity, this region is permeated by at most 1% connected partial melt: Fig. 8 shows predictions for mantle conductivities as a function of temperature and melt content using the SO2 model of Constable et al. (1992) for subsolidus olivine, and melt conductivities from Tyburczy and Waff (1983) (see also Roberts and Tyburczy, 1999). Conductivities resulting from mixing the two phases were predicted using the tube model of Grant and West (1965), which approximately represents well-connected melt along grain edges. We see that 100 Ωm mantle between 1400 and 1500 °C is at the solidus, with at most 0.5% connected melt. Allowing the region of lower seismic velocities to be 30 Ωm only increases the possible connected melt content to 1%. To explain the 5% anomaly in seismic velocities observed by Laske et al. (1999) in terms of partial melt would require melt fractions of 3–4% (Sato et al., 1989), which is unlikely given the high resistivities observed in this region; 3% melt would require 10 Ωm in the seismic low velocity region (LVR), which we have already shown to be incompatible with the MT data. However, again appealing to Sato et al. (1989), seismic velocities decrease 5% as the temperature is increased from about 0.9 to 1.0 times the melting temperature. This corresponds to about 200 K, which, with reference to Fig. 8, corresponds to about an order of magnitude in electrical conductivity, and is suggestive of an off-swell lithosphere of 1250 °C or lower with resistivities of 10^3 Ωm or higher, and a region corresponding to reduced seismic velocities which is at 1450 °C or higher with a resistivity of around 10^2 Ωm. We ran such a forward model, and the fits to the data are indeed acceptable (rms=1.58).

Totally disconnected melt would have a much smaller effect on electrical conductivity than connected melt, and could in principle explain both the seismic velocities and electrical conductivity data. However, it is generally considered that melt fractions of more than 1% will be connected, mobile, and gravitationally unstable (McKenzie and Bickle, 1988), and even disparate studies on fertile mantle indicate that melt fractions above 3% will be connected (Faul, 1997). Thus it may be possible that 3% unconnected melt is the cause of the seismic LVR and associated lack of electrical signature, but this represents an extreme interpretation.

Beneath the islands, our 2D and Larsen (1975) 1D inversions show a low resistivity (around 10 Ωm) structure in the top 150 km of the plume. Assuming that the plume beneath Hawaii has a core temperature of between 1300 and 1500 °C, then sub-solidus olivine conduction cannot explain the observed resistivities. An obvious candidate for reduced resistivities is the presence of melt at depths of up to 120 km. A melt fraction of 7% (White and McKenzie, 1995) implies a bulk resistivity of around 10 Ωm (Fig. 8), in good agreement with our results. Melt connection beneath Hawaii may be anisotropic, with higher vertical than horizontal conductivities, but there are too few data to pursue this problem at present. Above the seafloor, the islands also have low resistivity, perhaps due to high porosity filled with hot saline fluids.

Acknowledgments

We would like to thank the officers and crew of the RV Moana Wave for two excellent cruises in April and December, 1997. A. White, J. Phipps Morgan, G. Laske, L. MacGregor and K. Key contributed to various aspects of deployments and recoveries. A. White, B. Perkins and B. Walker at Flinders University, and J. Lemire and T. Deaton at Scripps Institution of Oceanography are thanked for support equipment design and construction. Two anonymous reviewers suggested improvements to the manuscript. G. Heinson was funded by the Australian Research Council. Funding under the National Science Foundation grant number OCE 95-29707 provided logistical support for the MT deployments.

References

Chave, A.D., Thomson, D.J., 1989. Some comments on magnetotelluric response function estimation. J. Geophys. Res. 94, 14215–14225.

Constable, S.C., Cox, C.S., 1996. Marine controlled source electromagnetic sounding: 2. The PEGASUS experiment. J. Geophys. Res. 101, 5519–5530.

Constable, S.C., Shankland, T.J., Duba, A., 1992. The electrical conductivity of an isotropic olivine mantle. J. Geophys. Res. 97, 3397–3404.

Constable, S.C., Orange, A.S., Hoverston, M.G., Morrison, F.H., 1998. Marine magnetotellurics for petroleum exploration: Part 1. A seafloor equipment system. Geophysics 63, 816–825.

Crough, S.T., 1978. Thermal origin of mid-plate hot-spot swells. Geophys. J. R. Astron. Soc. 55, 451–469.

deGroot-Hedlin, C., Constable, S.C., 1990. Occam's inversion to generate smooth two-dimensional models from magnetotelluric data. Geophysics 55, 1613–1624.

Detrick, R.S., Crough, S.T., 1978. Island subsidence, hot spot, and lithosphere thinning. J. Geophys. Res. 97, 2037–2070.

Faul, U., 1997. Permeability of partially molten upper mantle rocks from experiments and percolation theory. J. Geophys. Res. 102, 10299–10311.

Gordon, R.G., Jurdy, D.M., 1986. Cenozoic global plate motions. J. Geophys. Res. 91, 12389–12406.

Grant, F.S., West, G.F., 1965. Interpretation Theory in Applied Geophysics. McGraw-Hill, New York.

Groom, R.W., Bailey, R.C., 1989. Decomposition of magnetotelluric impedance tensors in the presence of local three-dimensional galvanic distortion. J. Geophys. Res. 94, 1193–1925.

Heinson, G.S., Constable, S.C., 1992. The electrical conductivity of the oceanic upper mantle. Geophys. J. Int. 110, 159–179.

Heinson, G., Constable, S., White, A., 2000. Episodic melt transport at a mid-ocean ridge inferred from magnetotelluric sounding. Geophys. Res. Lett. 27, 2317–2320.

Larsen, J.C., 1975. Low frequency (0.1–6.0 cpd) electromagnetic study of deep mantle electrical conductivity beneath the Hawaiian islands. Geophys. J. R. Astron. Soc. 43, 17–46.

Laske, G., Phipp Morgan, J., Orcutt, J.A., 1999. First results from the Hawaiian swell experiment. Geophys. Res. Lett. 26, 3397–3400.

Lilley, F.E.M., 1998. Magnetotelluric tensor decomposition: Part I. Theory for a basic procedure. Geophysics 63, 1885–1897.

Lilley, F.E.M., Arora, B.R., 1982. The sign convention for quadrature Parkinson arrows in geomagnetic induction studies. Rev. Geophys. Space Phys. 20, 513–518.

McKenzie, D., Bickle, M.J., 1988. The volume and composition of melt generated by extension of the lithosphere. J. Petrol. 29, 625–679.

McKirdy, D.M., Weaver, J.T., 1984. Induction in a thin sheet of variable conductance at the surface of a stratified earth: I. Two-dimensional theory. Geophys. J. R. Astron. Soc. 78, 93–103.

McKirdy, D.M., Weaver, J.T., Dawson, T.W., 1985. Induction in a thin sheet of variable conductance at the surface of a stratified earth: II. Three-dimensional theory. Geophys. J. R. Astron. Soc. 80, 177–194.

Neal, S.L., Mackie, R.L., Larsen, J.C., Schultz, A., 2000. Variations in the electrical conductivity of the upper mantle beneath North America and the Pacific Ocean. J. Geophys. Res. 105, 8229–8242.

Nolasco, R., Tarits, P., Filloux, J.H., Chave, A.D., 1998. Magnetotelluric imaging of the society islands hot spot. J. Geophys. Res. 103, 30287–30309.

Phipps Morgan, J., Morgan, W.J., Price, E., 1995. Hotspot melting generates both hotspot volcanism and a hotspot swell? J. Geophys. Res. 100, 8045–8062.

Ribe, N.M., Christensen, U.R., 1999. The dynamical origin of Hawaiian volcanism. Earth Planet. Sci. Lett. 171, 517–531.

Roberts, J.J., Tyburczy, J.A., 1999. Partial-melt electrical conductivity: influence of melt composition. J. Geophys. Res. 104, 7055–7065.

Robinson, E.M., 1988. The topographic and gravitational expression of density anomalies due to melt extraction in the uppermost oceanic upper mantle. Earth Planet. Sci. Lett. 90, 221–228.

Sato, H., Sacks, I.S., Murase, T., 1989. The use of laboratory velocity data for estimating temperature and partial melt fraction in the low-velocity zone: comparison with heat flow and electrical conductivity studies. J. Geophys. Res. 94, 5689–5704.

Simpson, F., Steveling, E., Leven, M., 2000. The effect of the Hawaiian plume on the magnetic daily variation. Geophys. Res. Lett. 27, 1775–1778.

Sleep, N.H., 1990. Hotspots and mantle plumes: some phenomenology. J. Geophys. Res. 95, 6715–6736.

Tyburczy, J.A., Waff, H.S., 1983. Electrical conductivity of molten basalt and andesite to 25 kilobars pressure: geophysical significance and implications for charge transport and melt structure. J. Geophys. Res. 88, 2413–2430.

von Herzen, R.P., Detrick, R.S., Crough, S.T., Epp, D., Fehn, U., 1982. Thermal origin of the Hawaiian swell: heat flow evidence and thermal models. J. Geophys. Res. 87, 6711–6723.

von Herzen, R.P., Cordery, M.J., Fang, C., Detrick, R.S., Fang, C., 1989. Heat flow and the thermal origin of hot spot swells: the Hawaiian swell revisited. J. Geophys. Res. 94, 13783–13800.

Wannamaker, P.E., Hohmann, G.W., Ward, S.H., 1984. Magnetotelluric responses of three-dimensional bodies in layered earths. Geophysics 49, 1517–1533.

Wannamaker, P.E., Stodt, J.A., Rijo, L., 1986. A stable finite element solution for two-dimensional magnetotelluric modelling. Geophys. J. R. Astron. Soc. 88, 277–296.

White, R.S., McKenzie, D.P., 1995. Mantle plumes and flood basalts. J. Geophys. Res. 100, 17543–17585.

Xu, Y.S., Shankland, T.J., Poe, B.T., 2000. Laboratory-based electrical conductivity in the earth's mantle. J. Geophys. Res. 105, 27865–27875.